

University of Wollongong

Research Online

Faculty of Engineering and Information
Sciences - Papers: Part A

Faculty of Engineering and Information
Sciences

1-1-2016

Design and development of a parametrically excited nonlinear energy harvester

Tanju Yildirim

University of Wollongong, ty370@uowmail.edu.au

Mergen H. Ghayesh

University of Adelaide, mergen.ghayesh@adelaide.edu.au

Weihua Li

University of Wollongong, weihuali@uow.edu.au

Gursel Alici

University of Wollongong, gursel@uow.edu.au

Follow this and additional works at: <https://ro.uow.edu.au/eispapers>



Part of the [Engineering Commons](#), and the [Science and Technology Studies Commons](#)

Recommended Citation

Yildirim, Tanju; Ghayesh, Mergen H.; Li, Weihua; and Alici, Gursel, "Design and development of a parametrically excited nonlinear energy harvester" (2016). *Faculty of Engineering and Information Sciences - Papers: Part A*. 5908.

<https://ro.uow.edu.au/eispapers/5908>

Research Online is the open access institutional repository for the University of Wollongong. For further information contact the UOW Library: research-pubs@uow.edu.au

Design and development of a parametrically excited nonlinear energy harvester

Abstract

An energy harvester has been designed, fabricated and tested based on the nonlinear dynamical response of a parametrically excited clamped-clamped beam with a central point-mass; magnets have been used as the central point-mass which pass through a coil when parametrically excited. Experiments have been conducted for the energy harvester when the system is excited (i) harmonically near the primary resonance; (ii) harmonically near the principal parametric resonance; (iii) by means of a non-smooth periodic excitation. An electrodynamic shaker was used to parametrically excite the system and the corresponding displacement of the magnet and output voltages of the coil were measured. It has been shown that the system displays linear behaviour at the primary resonance; however, at the principal parametric resonance, the motion characteristic of the magnet substantially changed displaying a strong softening-type nonlinearity. Theoretical simulations have also been conducted in order to verify the experimental results; the comparison between theory and experiment were within very good agreement of each other. The energy harvester developed in this paper is capable of harvesting energy close to the primary resonance as well as the principal parametric resonance; the frequency-band has been broadened significantly mainly due to the nonlinear effects as well as the parametric excitation.

Keywords

nonlinear, design, energy, development, harvester, parametrically, excited

Disciplines

Engineering | Science and Technology Studies

Publication Details

Yildirim, T., Ghayesh, M. H., Li, W. & Alici, G. (2016). Design and development of a parametrically excited nonlinear energy harvester. *Energy Conversion and Management*, 126 247-255.

Design and development of a parametrically excited nonlinear energy harvester

Tanju Yildirim ^a, Mergen H. Ghayesh ^b, Weihua Li ^a, Gursel Alici ^a

^a *School of Mechanical, Materials and Mechatronics Engineering, University of Wollongong, Northfields Avenue, NSW 2522, Australia*

^b *School of Mechanical Engineering, University of Adelaide, South Australia 5005, Australia*

Abstract

An energy harvester has been designed, fabricated and tested based on the nonlinear dynamical response of a parametrically excited clamped-clamped beam with a central point-mass; magnets have been used as the central point-mass which pass through a coil when parametrically excited. Experiments have been conducted for the energy harvester when the system is excited (i) harmonically near the primary resonance; (ii) harmonically near the principal parametric resonance; (iii) by means of a non-smooth periodic excitation. An electrodynamic shaker was used to parametrically excite the system and the corresponding displacement of the magnet and output voltages of the coil were measured. It has been shown that the system displays linear behaviour at the primary resonance; however, at the principal parametric resonance, the motion characteristic of the magnet substantially changed displaying a strong softening-type nonlinearity. Theoretical simulations have also been conducted in order to verify the experimental results; the comparison between theory and experiment were within very good agreement of each other. The energy harvester developed in this paper is capable of harvesting energy close to the primary resonance as well as the principal parametric resonance; the frequency-band has been broadened significantly mainly due to the nonlinear effects as well as the parametric excitation.

25 **Keywords**

26 Energy Harvesting; vibration based; Parametric Excitation; Experiment

27 **1. Introduction**

28 Due to increased demands for energy and current limitations of batteries, a future
29 prospective technology is motion based energy harvesters (MBEHs) that convert kinetic
30 energy into electrical energy [1]; this type of energy harvester has the potential to be used in
31 powering electronic devices in hostile or remote environments—another benefit of MBEH
32 devices is that they reduce pollutants in the environment which are left behind when batteries
33 are disposed.

34 For the transduction mechanisms used to convert kinetic energy into electrical power;
35 these can be grouped into *three* main categories. The first category uses piezoelectric
36 conversion, which converts mechanical strain into electrical energy; for instance, Adhikari et
37 al. [2] numerically investigated motion based energy harvesting under broadband excitation
38 using a stack configuration of piezoelectric energy harvesters—expressions were derived for
39 the non-dimensional time constant, electromechanical coupling coefficient and viscous
40 damping factor. Renno et al. [3] investigated into the optimised power that can be harvested
41 using a piezoelectric converter; using the Karush-Kuhn-Tucker technique, the power can be
42 substantially enhanced by using an optimal inductor in the load circuit. Fan et al. [4]
43 numerically and experimentally investigated the performance of a bi-directional nonlinear
44 piezoelectric energy harvester; to achieve a nonlinear frequency-voltage curve two embedded
45 magnets were used inducing a nonlinear stiffness—results showed that the bi-directional
46 energy harvester was more effective than its linear counterpart. Fan et al. [5] designed a
47 piezoelectric based energy harvester that could effectively harvest energy from sway and bi-

48 directional motions; using a cantilever beam, frame and roller a frequency-up conversion
49 mechanism was also achieved—results showed that the output voltage could be enhanced by
50 increasing the sway frequency. Guan et al. [6] recently developed a piezoelectric energy
51 harvester for rotational motion; a theoretical model was developed for the power output and
52 experimental results showed good agreement with the theory. The *second* category of
53 ambient motion energy harvesting transduction mechanisms are electrostatic conversion,
54 where capacitive plates fluctuate inducing a voltage; for example, Bu et al. [7] fabricated a
55 non-resonant wideband micro-energy harvester using electrostatic conversion—to boost low
56 frequency excitations, a parallel structure was used to double the output voltage. The *third*
57 mechanism that can be used to convert ambient kinetic energy into electrical power is
58 electromagnetic induction (EMI), where the relative motion between a magnet and coil
59 generates a backward electromotive force (EMF). For instance, Sardini et al. [8] developed a
60 low frequency energy harvester using polymeric material, due to their low Young’s modulus;
61 a theoretical and experimental investigation was conducted—results showed that a small
62 increase in bandwidth could be achieved with this design. Marin et al. [9] fabricated a linear
63 electromagnetic energy harvester with a four Hertz bandwidth using four cantilever beams
64 with closely related natural frequencies. Ooi et al. [10] designed a novel wideband
65 electromagnetic energy harvester using dual resonating cantilever beams; a numerical model
66 was done using MATLAB-Simulink; dual energy harvested peaks were observed resulting in
67 a slight increase in the devices bandwidth. Recently, Siddique [11] presented a
68 comprehensive review of micro-power generators using electromagnetic and piezoelectric
69 energy harvesters; a significant review of recent motion based energy harvesters were
70 compared to each other.

71 A major drawback with conventional MBEHs is the effective operating frequency
72 range which energy can be harvested; in practical applications, where the excitation

73 frequency is changing or varying with time, precisely matching the natural frequency of a
74 device is crucial for operation and can be achieved with tuning techniques, however, the
75 power required to tune a device will never result in greater energy harvested [12]. There are
76 two main classes for MBEH devices based on the core element being used; the first class
77 employs *linear* resonators and the second class uses *nonlinear* resonators.

78 For the *first* class, i.e. the *linear* energy harvesters, the maximum energy harvested is
79 achieved when the excitation frequency matches the primary natural frequency of the core
80 element in the MBEH device. The literature regarding this class is quite large. For instance,
81 William and Yates [13] first investigated the use of external resonating devices for powering
82 micro electrical mechanical systems (MEMS); this work was further theoretically extended
83 by Mitcheson et al. [14] for three different damping based resonators. Stephen [15]
84 theoretically investigated the potential of linear MBEH devices for direct mass and base
85 excitations, including the coupling between mechanical and electrical domains. Shahruz [16]
86 developed a multimodal array based on transversely excited cantilever beams with different
87 geometries and tip masses; the results showed that the combination of these linear energy
88 harvesters could achieve a larger bandwidth, however, the required circuitry was more
89 complex. Tang and Zuo [17] theoretically analysed dual mass linear resonators to widen the
90 bandwidth of MBEH devices; dual mass devices could have two local optimums which can
91 further increase the bandwidth of the device. Erturk and Inman [18] further investigated
92 transversely excited linear cantilever beams with piezoelectric bimorph layers, using Euler-
93 Bernoulli beam theory for use as an energy harvester. Leland and Wright [19] designed a
94 linear MBEH device that could be tuned with compressive axial preloading further extending
95 the operating bandwidth of the energy harvester; other tuneable linear resonators based on
96 preloading mechanisms for energy harvesters have also been developed for example in [20].

97 The *second* class of MBEHs can be divided into *two sub-classes*, there are: energy
98 harvesters whose core elements are either *transversely* excited or *parametrically* excited; for
99 the transversely excited system, there is a large volume of available literature. For instance,
100 Mann and Simms [21] fabricated a nonlinear energy harvester based on the transverse
101 oscillation of a levitated magnet; a perturbation technique known as the method of multiple
102 scales was employed to derive the theoretical frequency response curve—experimental and
103 theoretical results were within good agreement. Maiorca et al. [22] and Liu et al. [23]
104 fabricated MBEH devices utilising mechanical stoppers in which both devices showed
105 nonlinear energy extraction near the primary resonance. Sebald et al. [24] analysed the effects
106 of magnetically induced nonlinearities in transversely excited cantilever beams with
107 piezoelectric layers experimentally. In general, bi-stable energy harvesters have a broader
108 bandwidth [25] and the energy harvested is not influenced under white noise [26].

109 The literature on the *second* sub-group (of the second class), which are *nonlinear*
110 energy harvesters based on *parametric* excitations of their core elements, is not extensive; for
111 example, Abdelkefi et al. [27] theoretically investigated a parametrically excited cantilever
112 beam for energy harvesting purposes using the Galerkin discretisation and the method of
113 multiple scales; the modelling also includes geometric, inertial and piezoelectric
114 nonlinearities. Daqaq et al. [28] investigated the applicability of parametric energy harvesting
115 with large emphasis on the theoretical model using a perturbation technique; experiments
116 were also conducted on a cantilevered beam with a tip mass—this system showed a *weak*
117 softening-type nonlinearity in the vicinity of the principal parametric resonance.

118 In this paper, for the first time, an energy harvester has been developed and tested
119 experimentally based on the nonlinear dynamical behaviour of a *parametrically excited beam*
120 *carrying a point-mass* as the core element subject to a magnetic field. The experiments
121 showed that the fabricated device has an *extended bandwidth* for effectively harvesting

122 kinetic energy; in particular, at the principal parametric resonance, the device displays a
123 *strong* softening-type nonlinearity at higher frequencies which is used to further maximise the
124 frequency band-width and hence kinetic energy harvested from the device—the device
125 harvests energy at *both* the primary and principal-parametric resonances. The energy
126 harvester designed based on *parametric excitation* is shown to *harvest energy over larger*
127 *frequency bands* due to the qualitative and quantitative changes in the *nonlinear dynamical*
128 *behaviour* of the core element. The paper has been organised as follows: a description of the
129 system including the fabricated device, background theory and experimental procedure are
130 developed in Section 2; the experimentally obtained results for the fabricated energy
131 harvester are acquired and discussed in detail in Section 3. Theoretical verifications are
132 provided in Section 4. Section 5 ends with concluding remarks.

133 **2. System description and experimental procedure**

134 This section describes the specifications of the energy harvester fabricated using a
135 parametrically excited beam carrying a concentrated mass as the core element as well as the
136 experimental setup and data recording and analysing system.

137 **2.1 System description**

138

139 The system shown in Fig.1 is the core element of an energy harvester with a
140 parametrically excited beam carrying a point-mass as the core element; one of the clamps is
141 fixed while the other is a moveable support in the longitudinal direction. An aluminium beam
142 with length L , width b and thickness h has dimensions of 160, 12, 0.6mm, respectively; a
143 magnet has been attached to either side of the centre of the beam with a net weight of 0.0196
144 kg (m) (as the concentrated mass). A coil was used as the transduction method to convert the
145 dynamic motion into the electrical energy through electromagnetic induction (EMI); the coil

146 consisted of 600 tightly wound turns and had an internal resistance of 2.7 Ohms. The open-
147 circuit voltage was measured during the experiments when the shaker was exciting the energy
148 harvester (see Figure 2); the moveable support was achieved by using linear bearings.

149 **2.2 Theoretical background**

150

151 A parametrically excited perfect system displays a zero-response throughout the
152 frequency space, the non-zero response emerges from the zero-response in the vicinity of the
153 principal parametric resonance; however, an initial threshold is required to activate a
154 parametric resonance—a characteristic parametric equation is known as the Mathieu equation
155 given by

$$156 \quad \ddot{x} + \alpha x^3 + [\omega - 2q \cos(2t)]x = 0, \quad (1)$$

157 where x is the displacement field, ω is the natural frequency, q is the forcing amplitude, α is
158 the nonlinear stiffness coefficient and t is the time. Understanding Eq. (1) from a design
159 perspectives means that energy can be harvested effectively from an imperfect system at two
160 frequencies that are relatively close to each other (depending on system parameters);
161 furthermore, the nonlinear stiffness term can be designed for using geometric extensibility at
162 the centreline of the core element resulting in nonlinear behaviour and hence nonlinear
163 frequency-response curves which will be further used to extend the operating bandwidth of
164 the fabricated energy harvester. For the energy harvester shown in Fig.1, ambient kinetic
165 energy is harvested using EMI; as the magnet passes through the coil an induced back
166 electromotive force is generated in the coil resulting in the conversion of kinetic energy into
167 electrical energy. The electromotive force generated is proportional to the rate of change in
168 the magnetic flux given by [29]

169 $V_{EMF} = -\frac{d\phi}{dt},$ (2)

170 where V_{EMF} is the back electromotive force and ϕ is the magnetic field flux density. For a
 171 uniform coil, the back EMF is proportional to the number of turns by [30]

172 $V_{EMF} = -N \frac{d\phi}{dt},$ (3)

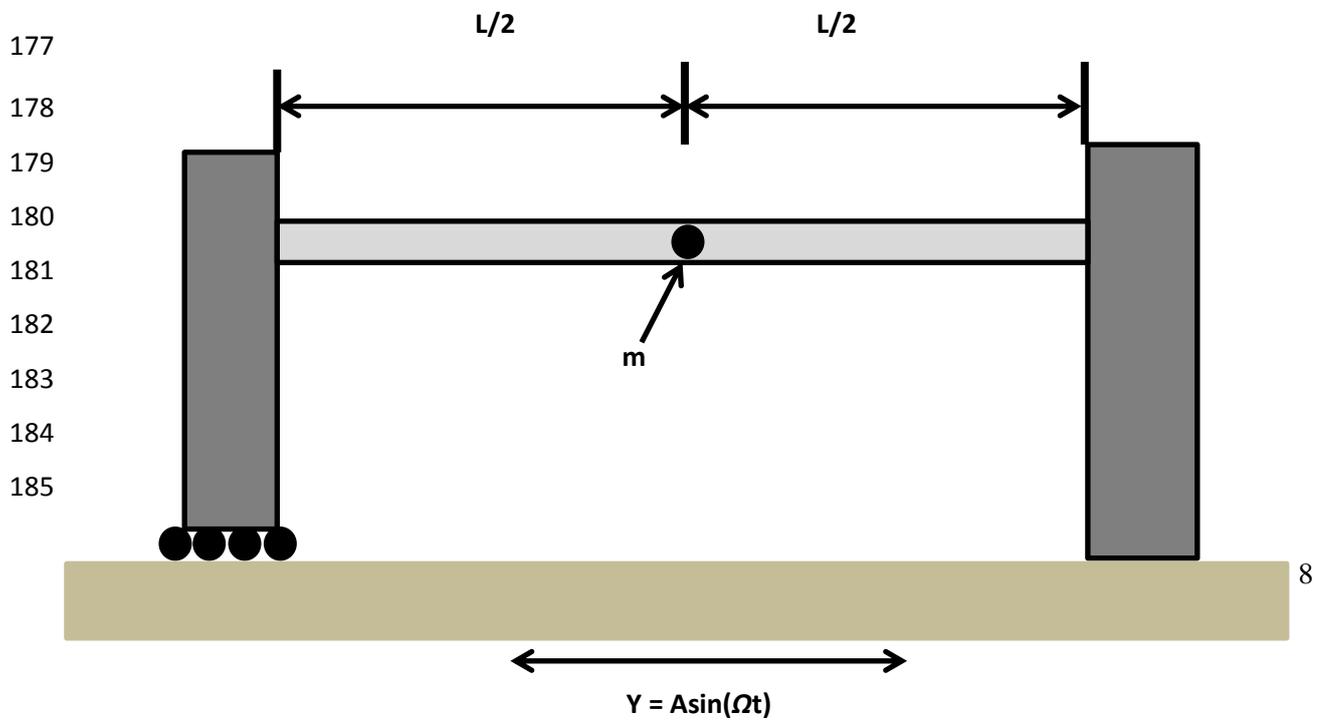
173 where N is the number of coil turns.

174 (a)



175

176 (b)



186

187

188

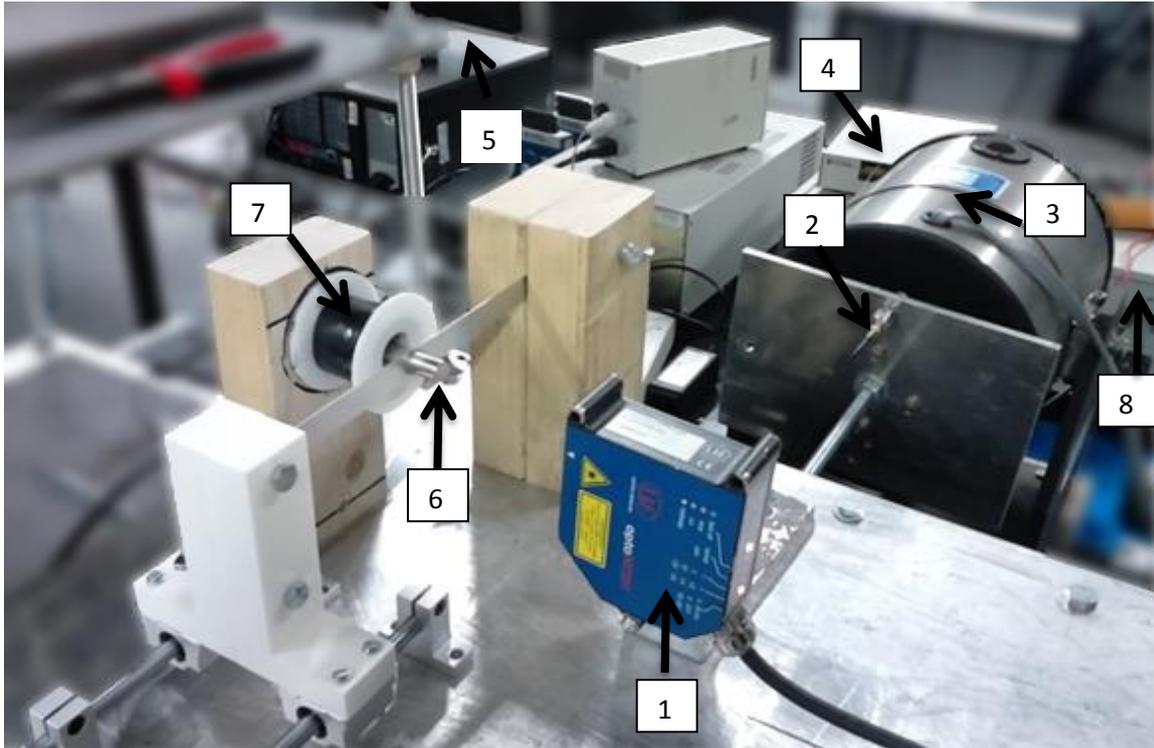
189 Figure 1: (a) A parametrically excited clamped-clamped beam carrying a concentrated mass as the core element of the
190 energy harvester; (b) Schematic of (a)

191 **2.3 Experimental procedure**

192

193 Figure 2 shows the experimental setup and the connection between system components,
194 for measuring and acquiring experimental data for analysis. The beam was excited using an
195 electrodynamic shaker (VTS, VC 100-8); the corresponding displacement of the central
196 magnet was measured using a laser displacement sensor (Microepsilon opto
197 NCDT1700ILD1700-50) and the output voltage of the coil was measured through a data
198 acquisition board (DAQ National instruments PCI-6221). The closed loop control system was
199 achieved using an accelerometer (CA YD106) connected to the electrodynamic shaker to
200 control the base excitation amplitude; the output voltage of the DAQ board was enlarged
201 through a power amplifier (Sinocera YE5871).

202 The system was excited in the horizontal plane and the resulting motion of the magnets
203 was 90^0 (perpendicular) to the base excitation; a swept sine signal in the form of $Y = A\sin(\Omega t)$
204 (with A and Ω being the acceleration amplitude and frequency) using LABVIEW software
205 was implemented to test the energy harvester.



206

207
208

Figure 2: Photograph of the experimental setup (1. Laser Displacement Sensor; 2. Accelerometer; 3. Electrodynamic shaker; 4. DAQ board; 5. Computer; 6. Magnet; 7. Coil; 8. Power amplifier)

209

210 3. Experimental results for energy harvested

211

212 The fabricated energy harvester using a beam carrying a central mass as the core
 213 element was experimentally tested when the system was excited (i) harmonically near the
 214 primary resonance; (ii) harmonically near the principal resonance; (iii) near the principal
 215 resonance with a non-smooth periodic function. Experiments (i-iii) were used to *qualitatively*
 216 and *quantitatively* investigate the *nonlinear dynamical response* of the *parametric resonator*
 217 under different acceleration amplitudes to determine the MBEH devices *broader operating*
 218 *range*. A non-dimensional frequency has been introduced as the excitation frequency divided
 219 by the experimentally obtained fundamental primary linear resonance of the energy harvester
 220 (Ω/ω_1) and at the principal parametric resonance ($\Omega/2\omega_1$); similarly, a non-dimensional
 motion amplitude has been introduced as the parametric motion amplitude divided by the

221 thickness of the beam (Displacement/h). The experimentally obtained results for the
222 displacement and voltage are presented; referring to Fig.2, the positive motion amplitude and
223 voltage occur when the magnet is moving away from the displacement sensor and the
224 negative motion amplitude and voltage occur when the magnet moves toward the
225 displacement sensor. The frequency-response curves, time traces, fast Fourier transform
226 (FFT), phase-plane diagrams and probability density function (PDF), for experiments (ii) and
227 (iii) are experimentally obtained and plotted to describe the *nonlinear dynamical response*
228 and hence the *nonlinear energy harvested*; the frequency-response curve for the open-circuit
229 voltage of the energy harvester are also experimentally acquired and plotted.

230

231 **3.1 Energy harvested in the vicinity of the primary resonance**

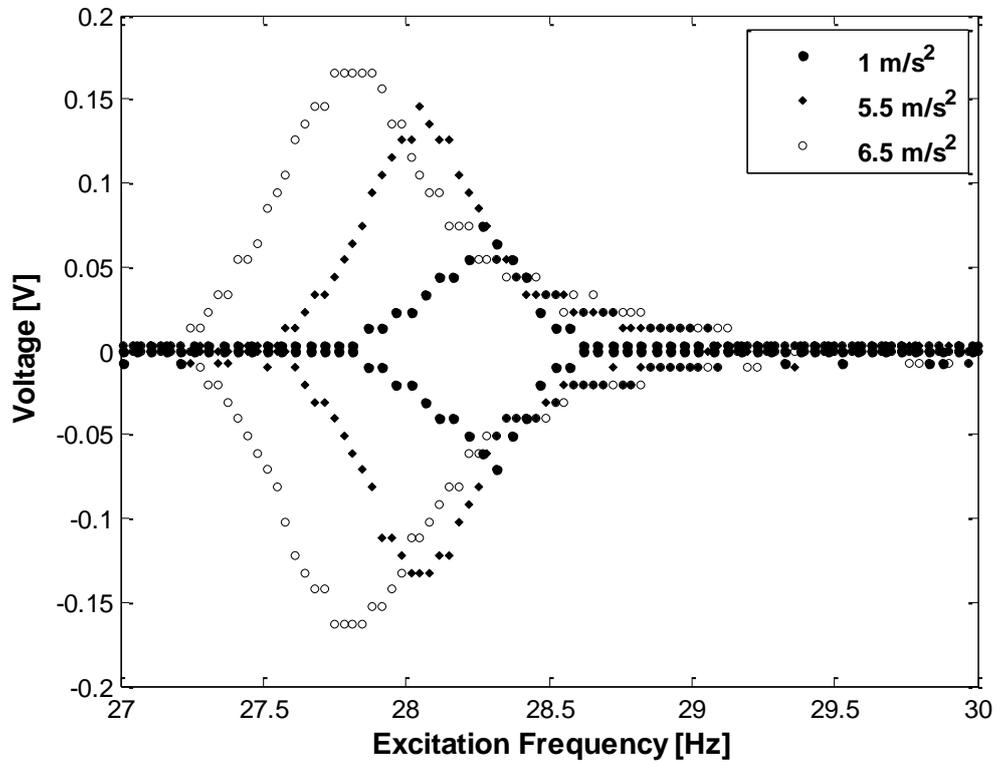
232

233 In this section, experiments have been conducted in order to analyse the response of
234 the energy harvester when excited in the vicinity of the *primary resonance* of the core
235 element; results are plotted for both the energy harvested and motion characteristics of the
236 resonator.

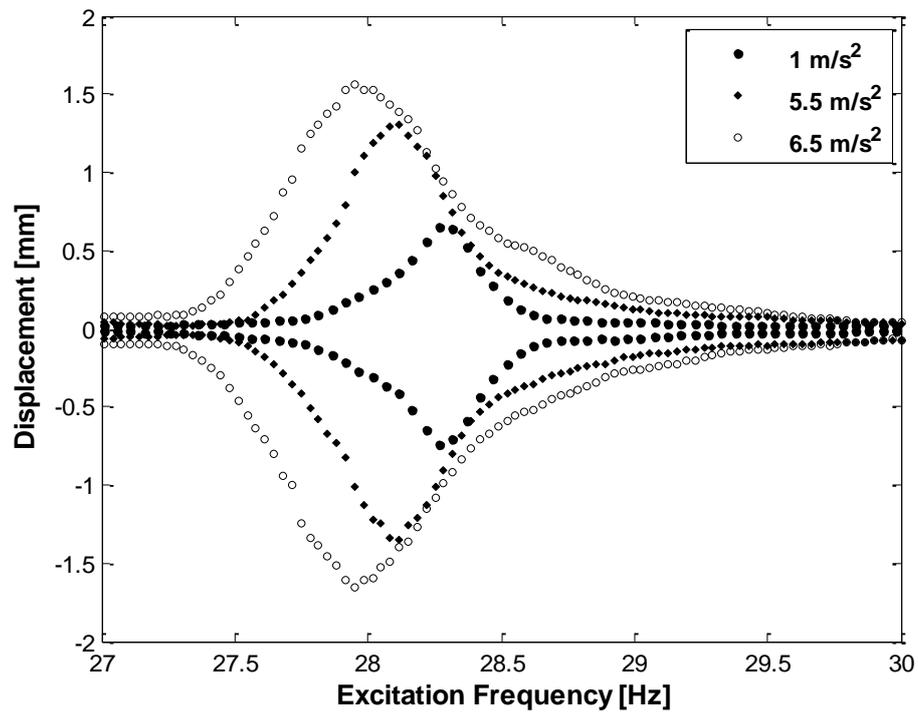
237 Figures 3(a)–(c) show the open-circuit voltage measured from the coil, the
238 dimensioned displacement of the central mass and the non-dimensioned motion amplitude of
239 the central mass, respectively. It was observed that there was a slight shift in the primary
240 resonance at different excitation amplitudes; this was due to slight initial geometric
241 imperfections in the beam—the corresponding primary resonance frequencies for 1, 5.5, 6.5
242 ms^{-2} excitation amplitudes were experimentally obtained as 28.27, 28.12 and 27.95 Hz,
243 respectively. When the energy harvester was excited near the primary resonance, a linear
244 response was observed characterised by a gradual incline to a maximum at Ω/ω_1 followed by
245 a gradual and continuous decline; no jump phenomenon was observed. It was also shown in

246 Fig.3 (a) that the open-circuit voltage was generated in the primary resonance region is
247 proportional to the relative displacement of the magnet and the coil.

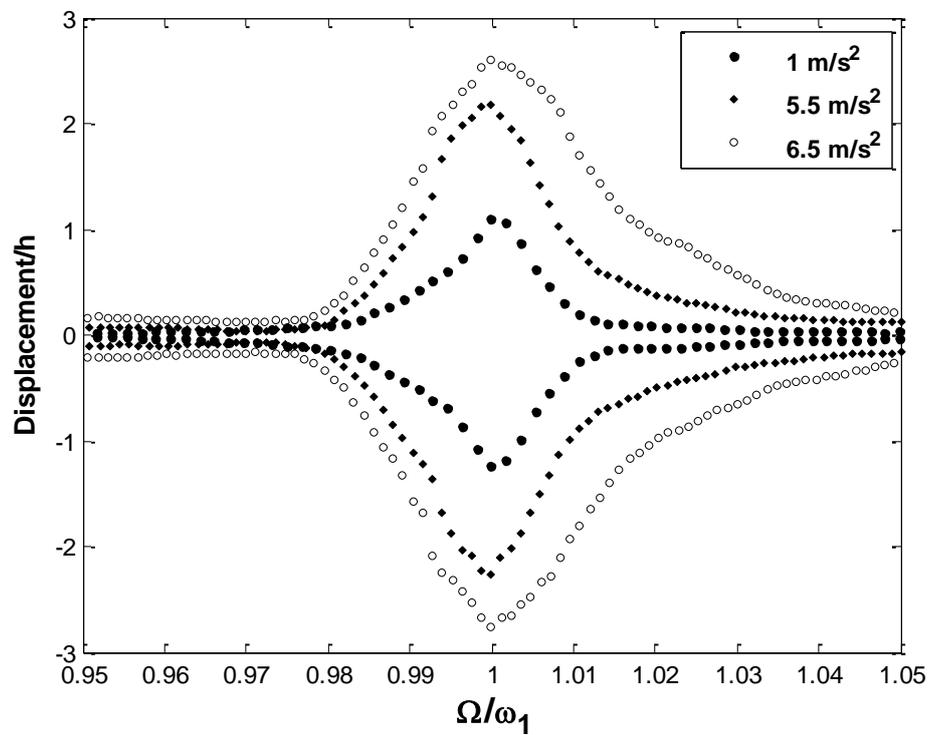
(a)



(b)



(c)



248
249

Figure 3: Frequency-response curves for the energy harvester in the vicinity of the primary resonance (a) Open-circuit voltage generated; (b) Dimensional displacement; (c) Non-dimensional displacement

250

251 **3.2 Energy harvested in the vicinity of the principal parametric resonance**

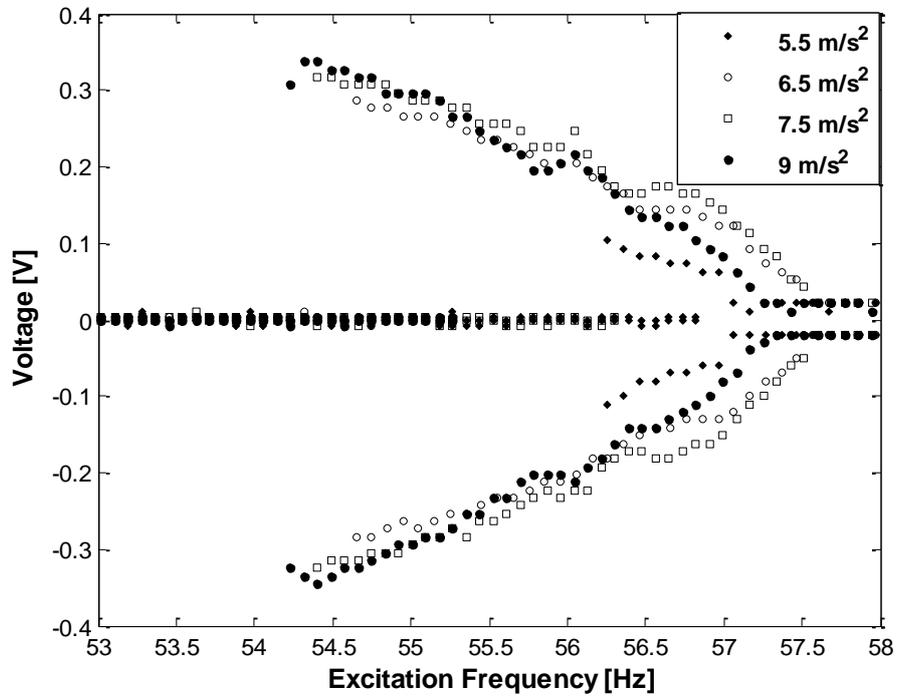
252

253 In this section, the nonlinear energy harvested from the energy harvester is
254 experimentally obtained when the nonlinear core element was excited in the vicinity of the
255 *principal parametric resonance*; the experimentally obtained results were plotted in Fig. 4
256 and are discussed in the following.

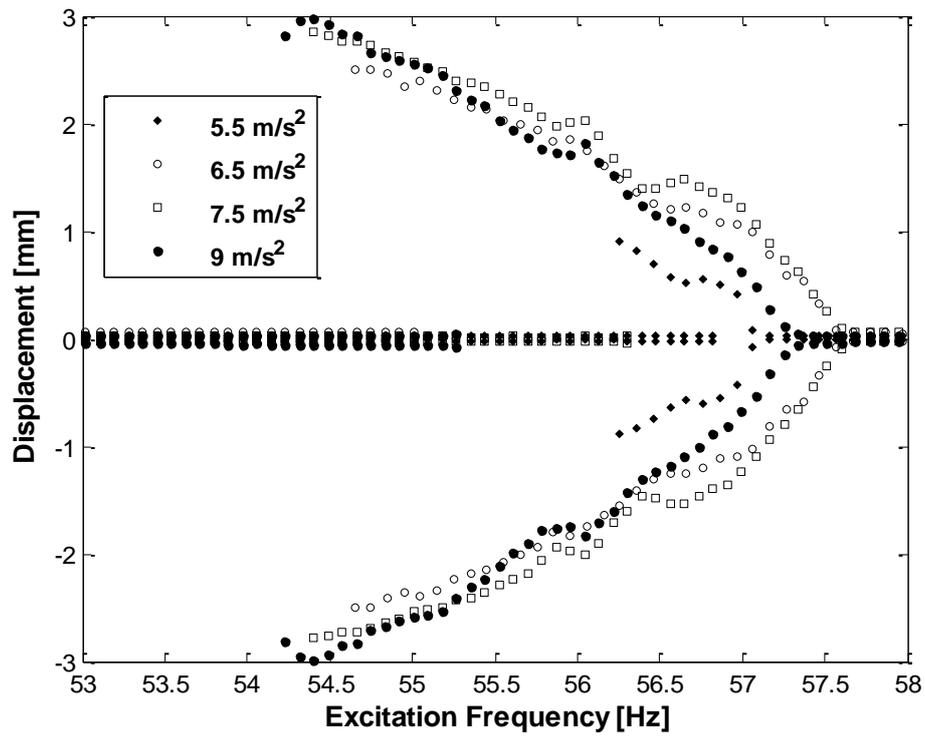
257 It is shown in Fig. 4 that when the energy harvester is excited in the vicinity of the
258 principal parametric resonance of the core element, the system displays a strong softening-
259 type nonlinearity bifurcated from a near-zero response; the softening behaviour can be
260 explained due to initial geometric imperfections in the fabrication process which is realistic in
261 manufacturing processes. Moreover, Fig. 4 displays a nonlinear dynamical behaviour
262 characterised by having two discontinuous points, theoretically these discontinuous points are
263 limit point and period-doubling bifurcations and experimentally these points occur as jump
264 down and jump up points or sudden growth in the response; there are two responses at a
265 specific excitation frequency which are the result of combing the forward and reverse
266 frequency sweeps. The system shows substantially different energy harvested and motion
267 characteristics compared to conventional *linear* energy harvesters in the literature, thus,
268 requiring a *nonlinear* analysis. It is shown in Fig.4(a) that the nonlinear energy extracted in
269 the vicinity of the principal parametric resonance improves the operating bandwidth of the
270 energy harvester and the maximum energy harvested; it was observed that an 11.5% energy
271 harvesting frequency band was achieved—it was also observed that there was a significant
272 increase in the maximum open-circuit voltage by about 300%, between, 5.5 and 6.5 ms⁻² base
273 excitation. For the maximum motion amplitude occurring at 54 Hz for 9 ms⁻² excitation
274 amplitude, the time trace, FFT, phase-plane diagram and PDF are shown in Figs.5(a)–(d),

275 respectively, showing a period-2 motion; however, the system is slightly non-symmetric
276 which is due to the initial geometric imperfection.

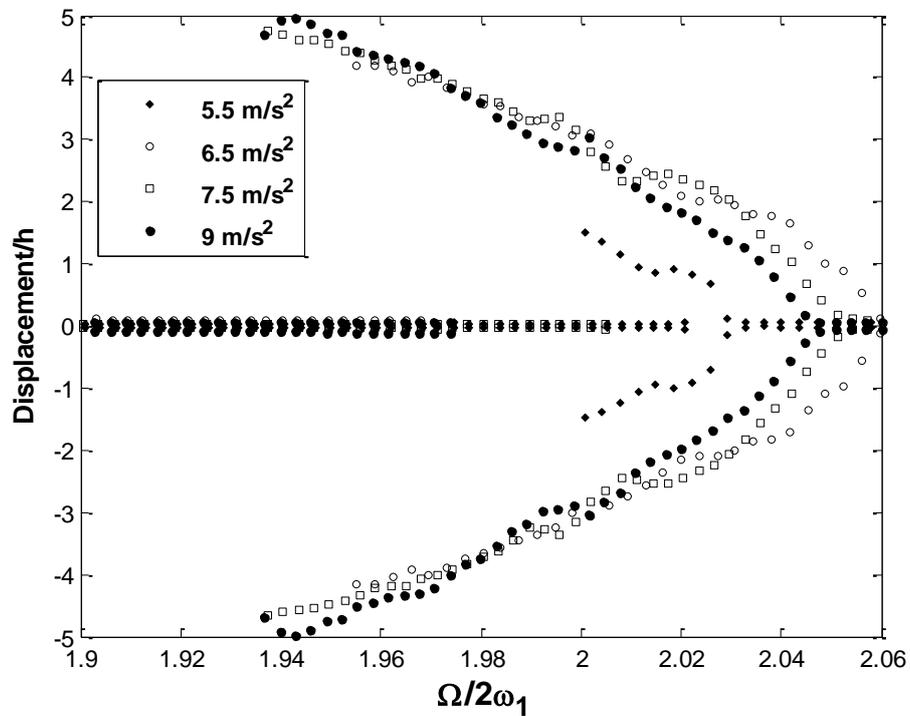
(a)



(b)

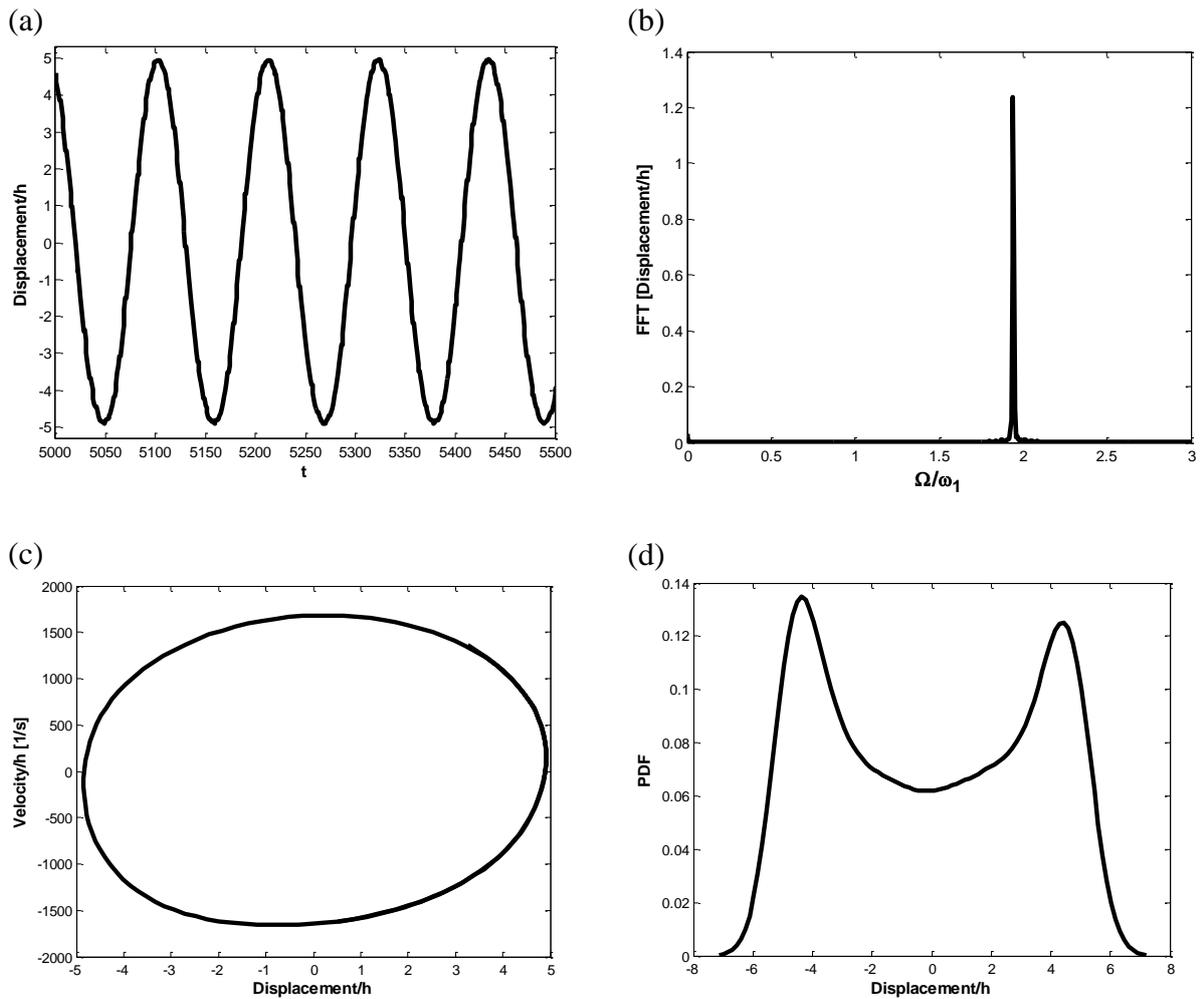


(c)



277
278

Figure 4: Frequency-response curves for the energy harvester in the vicinity of the principal parametric resonance (a) Open-circuit voltage generated; (b) Dimensional displacement; (c) Non-dimensional displacement



279

280 Figure 5: (a) Time trace; (b) FFT; (c) Phase plane diagram; (d) PDF at $\Omega = 54$ Hz and 9ms^{-2} base excitation, for the system
 281 of Fig. 4, illustrating a period-2 motion

282

283 3.3 Energy harvested from a non-smooth periodic excitation

284

285 In this section, a non-smooth periodic excitation has been generated by the shaker and
 286 applied to the base of the energy harvester; the *nonlinear energy harvested* as well as the
 287 *nonlinear dynamical response* are obtained experimentally and plotted.

288 Figure 6 illustrates the non-smooth periodic excitation signal from the electrodynamic
 289 shaker where Sub-figures 6 (a) and (b) show the time trace and FFT, respectively (there is
 290 noise along with a strong periodic component); the input signal is controlled through the
 291 accelerometer attached to the shaker (see Figure 2).

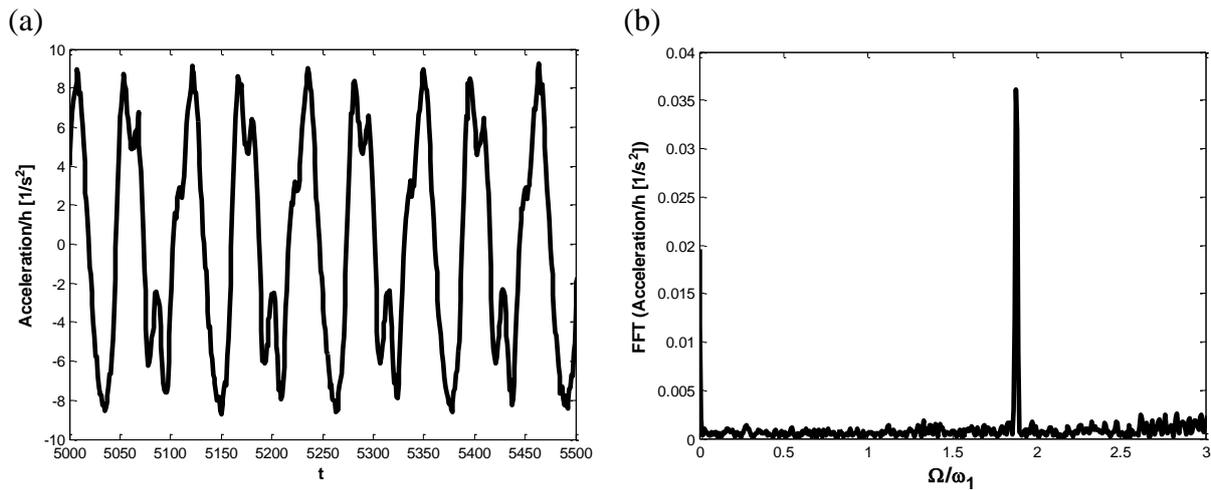


Figure 6: (a) Time trace; (b) FFT of input signal from electrodynamic shaker

292

293

294 Figure 7 shows the nonlinear voltage harvested (a), the dimensional nonlinear response (b)
 295 and the dimensionless nonlinear response (c); the energy harvester still displays a strong
 296 softening-type nonlinearity with discontinuous points occurring in the forward and reverse
 297 frequency sweeps at $\Omega = 56.36$ and 52.43 Hz, respectively. Comparing Figs. 7 and 4 (with
 298 non-smooth and smooth periodic excitations, respectively), the energy harvester performs
 299 better for non-smooth periodic excitations than with purely harmonic sinusoids which are
 300 more realistic in practical implementation; moreover, the effective operating bandwidth is
 301 increased over 20% and a maximum open-circuit voltage of 0.5V is harvested at 52.53 Hz.
 302 There are also traces of weak internal resonances present, for instance, in the vicinity of $\Omega =$
 303 53.94 and 54.55 Hz. The experimentally obtained time trace, FFT, phase-plane diagram and
 304 PDF are plotted in Figs.8(a)–(d) for $\Omega = 52.52$ Hz; the energy harvester displays a period-2
 305 motion which is slightly non-symmetric due to the initial geometric imperfections.

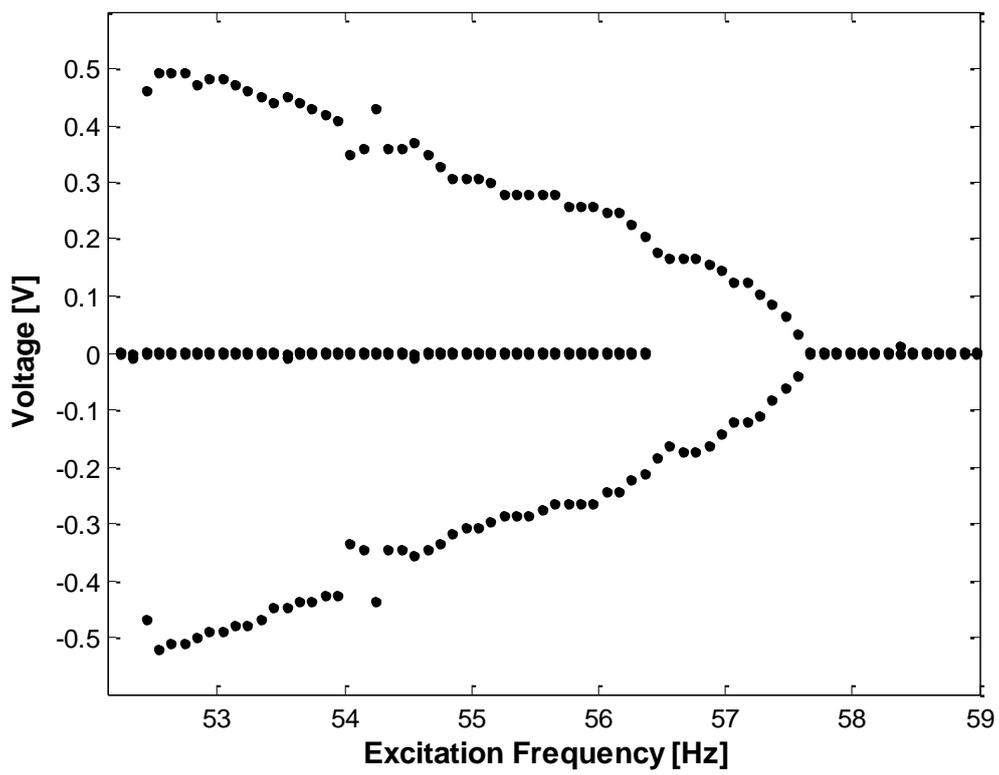
306

307

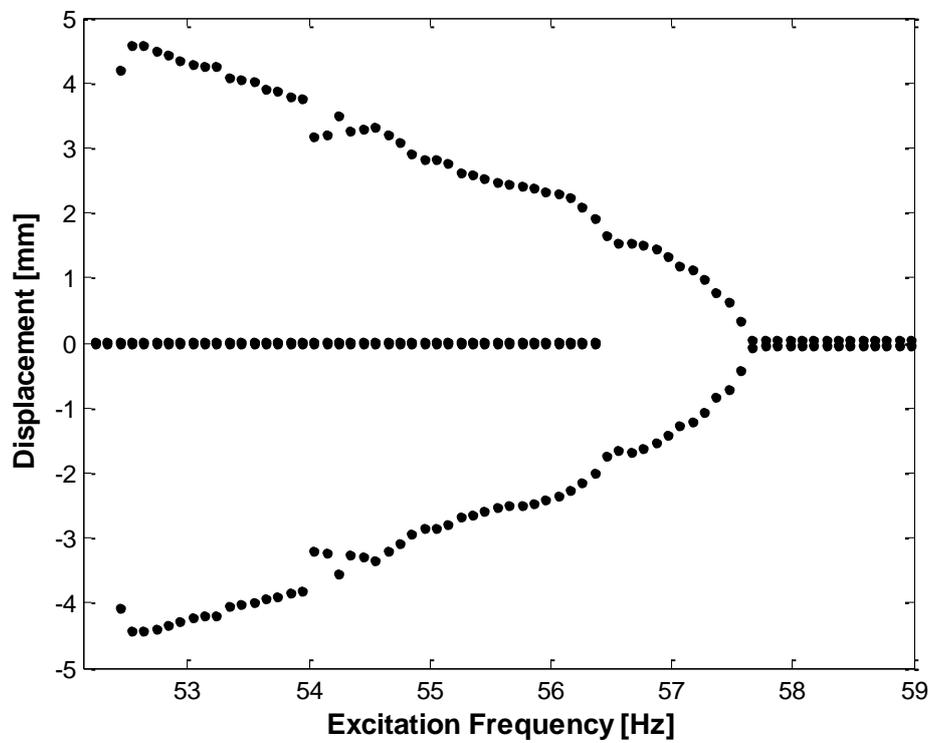
308

309

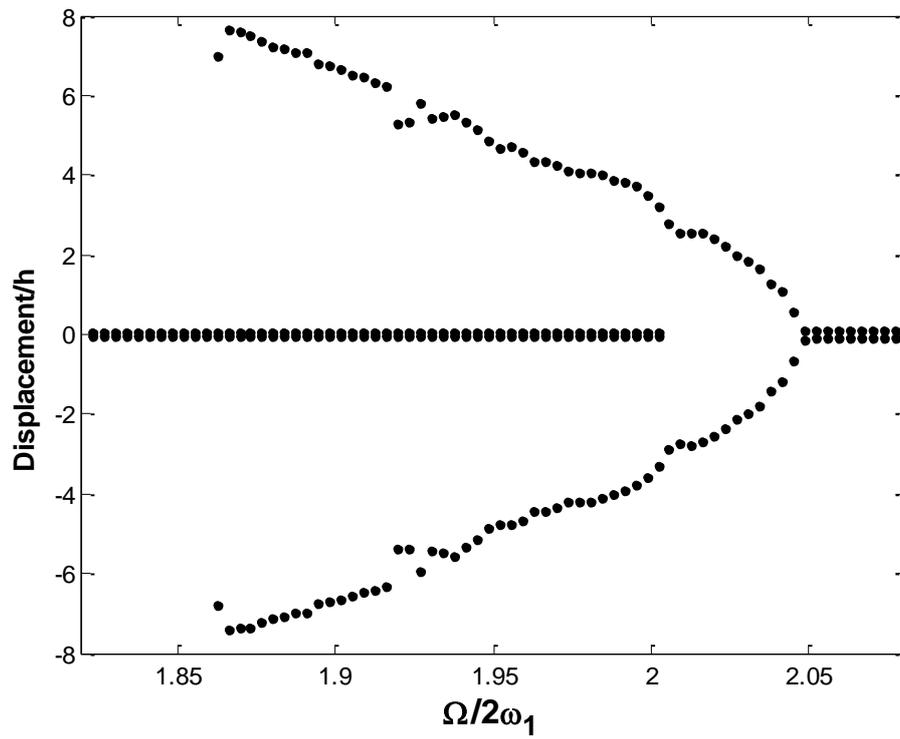
(a)



(b)



(c)



310 Figure 7: Frequency-response curves for the energy harvester in the vicinity of the primary resonance (a) Open-circuit
311 voltage generated; (b) Dimensional displacement; (c) Non-dimensional displacement

312

313

314

315

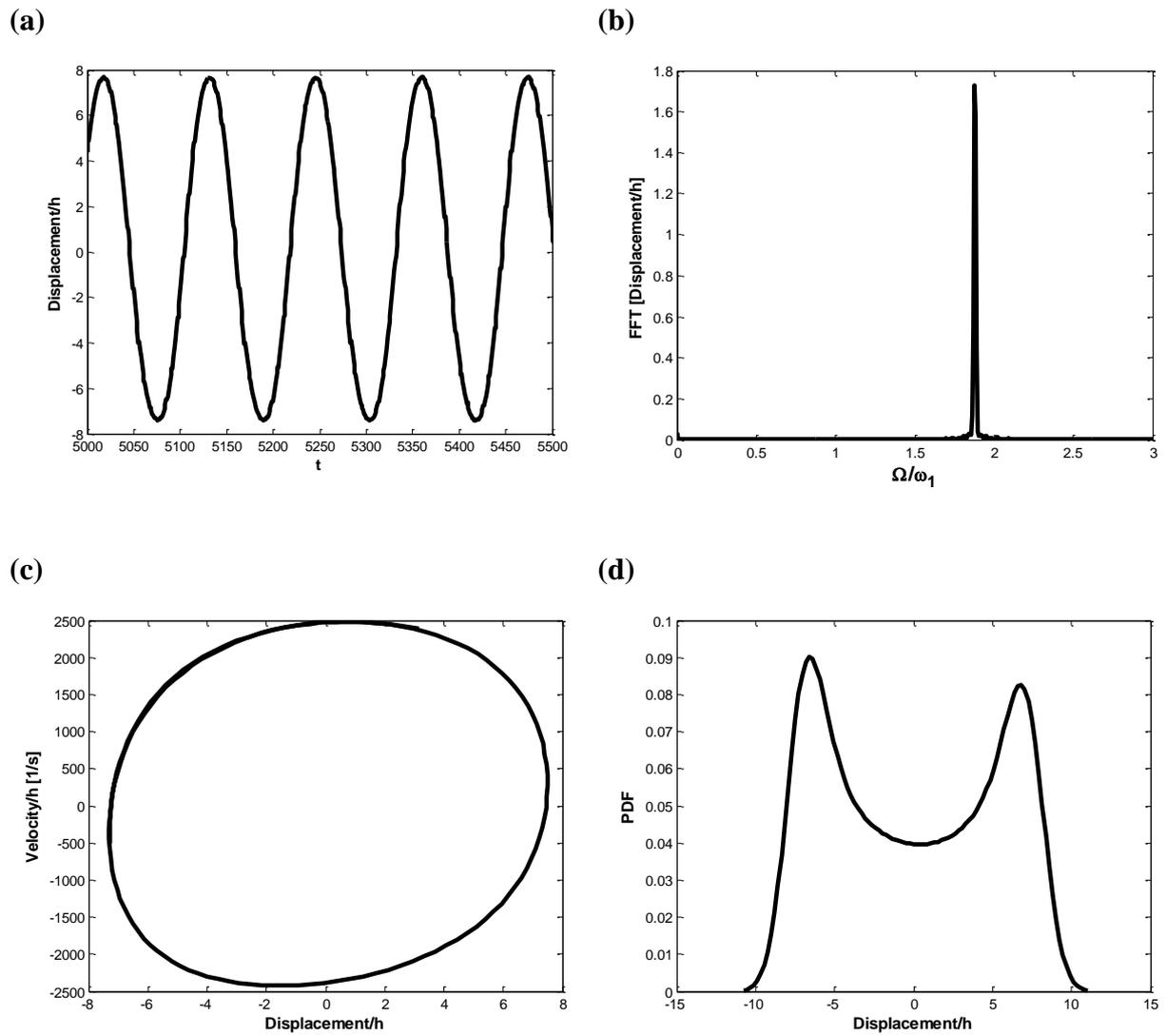
316

317

318

319

320



321 Figure 8: (a) Time trace; (b) FFT; (c) Phase plane diagram; (d) PDF at $\Omega = 52.53$ Hz, for the system of Fig. 7, illustrating a
 322 period-2 motion

323

324

Table 1: Comparison of the excitation types

Excitation	Bandwidth [Hz]	Max. Open Circuit Voltage [V]	Max. Displacement/h
Harmonic	3.02	0.34	4.96
Non-smooth periodic	5.24	0.52	7.624

325

326

327

328

A comparison of the two different excitation types, i.e. harmonic and non-smooth periodic is shown in Table 1. For the comparisons, the harmonic excitation was selected at 9 m/s^2 from Fig. 4; while for the non-smooth periodic excitation case, the system shown in Fig.

329 7 has been used because it has a maximum base excitation of 9 m/s^2 (which is the same as the
330 harmonic case). It was observed that under a non-smooth periodic excitation the fabricated
331 energy harvester has a larger bandwidth of 2.22 Hz compared to the harmonic excitation
332 case; this result was due to the non-smooth excitation causing more instability of the core
333 element which in turn activates motion attractors which are more beneficial for harvesting
334 energy.

335 **3.4 Acceleration-response curves**

336

337 To further demonstrate the nonlinear parametric behaviour, experiments were also
338 conducted for the acceleration-response curves at a fixed frequency of 56 Hz; this was done
339 as a design requirement to verify the minimum parametric threshold amplitude required to
340 activate a principal parametric resonance as shown in Figure 9. It was observed there are two
341 distinct discontinuous bifurcations at $Y = 4.525 \text{ m/s}^2$ and at $Y = 5.56 \text{ m/s}^2$; moreover, this
342 behaviour was due to the geometric extensibility at the centreline of the core element, the
343 geometric imperfection and the parametric excitation which have all been used in the design
344 of the fabricated energy harvester to further enhance the operating bandwidth of the device.

345

346

347

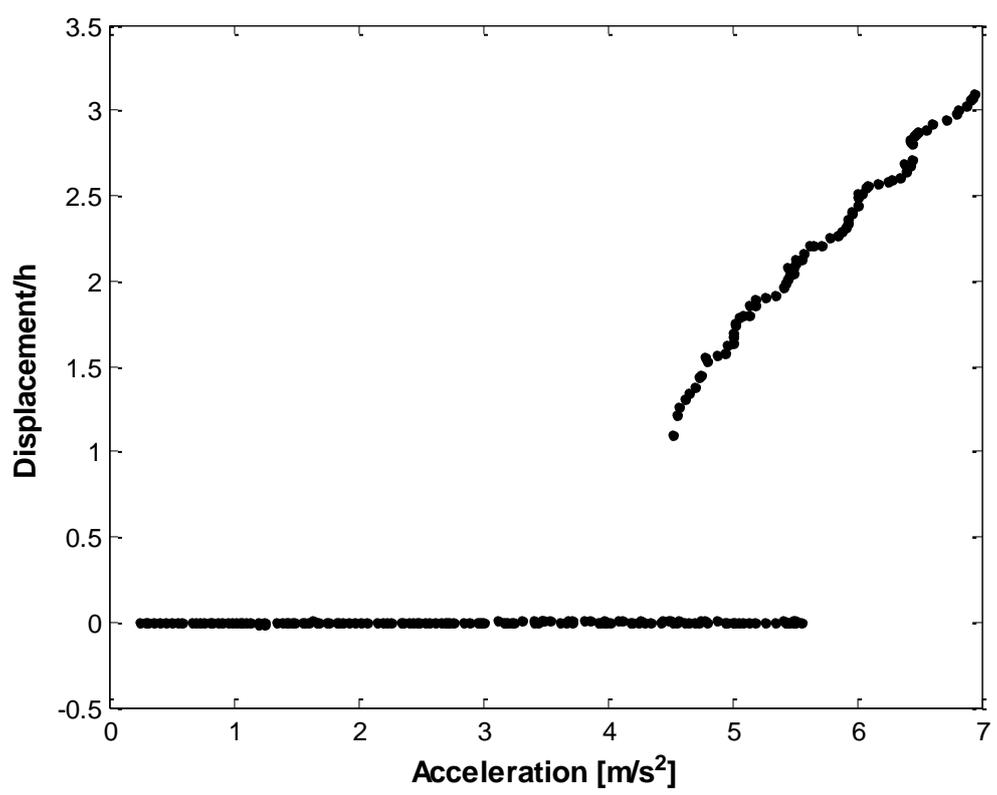
348

349

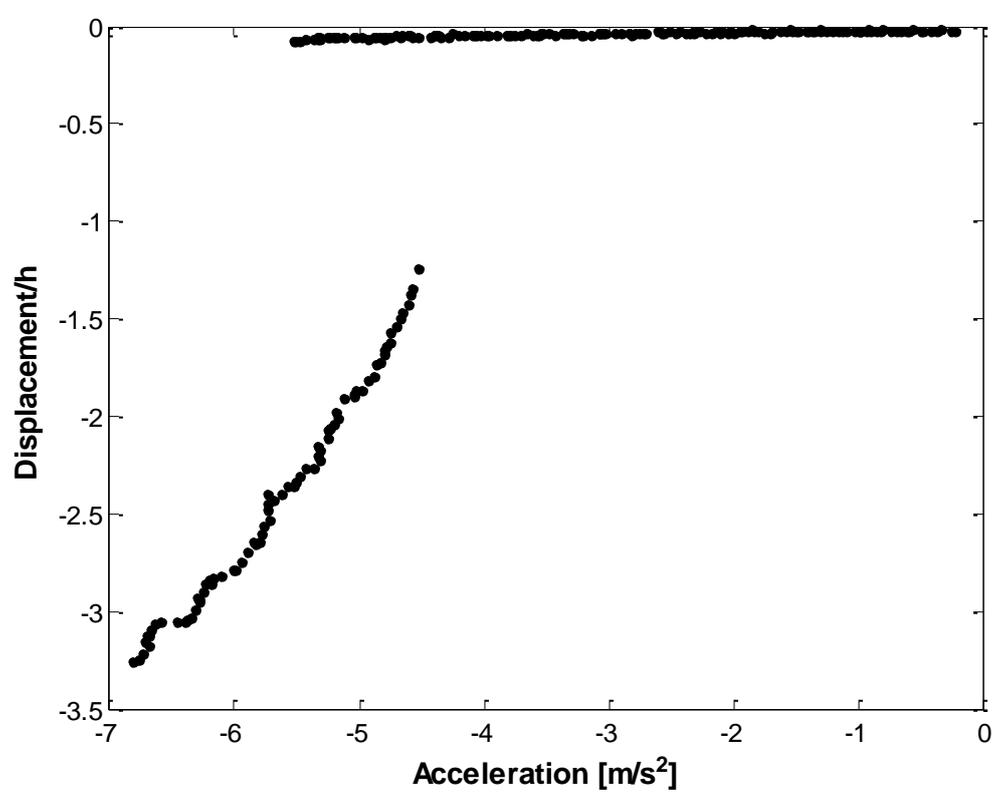
350

351

(a)



(b)

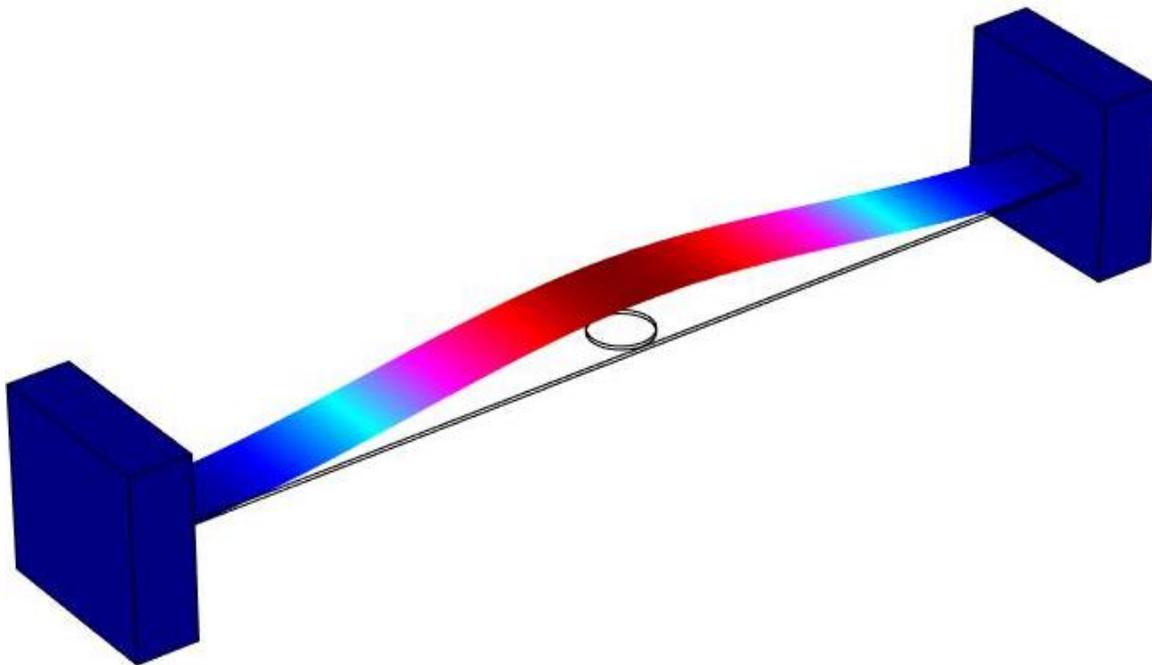


352
353

Figure 9: Acceleration-response curves for the core element at 56 Hz (a) Positive displacement (i.e. when moving away from the laser displacement sensor); (b) Negative displacement (i.e. when moving towards the laser displacement sensor)

354 4. Theoretical verification

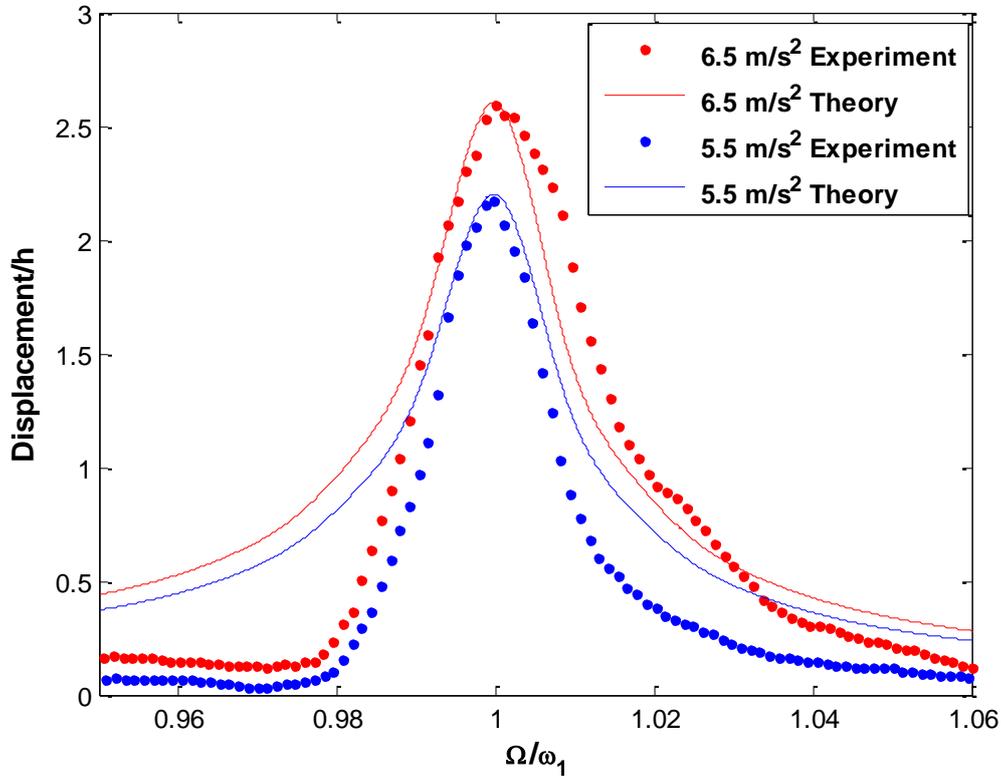
355 In this section, theoretical verifications of the experimentally obtained data has been
356 conducted. COMSOL Multiphysics 5.1, using the solid mechanics module, has been used for
357 the theoretical verifications; a geometry based on the schematic shown in sub-Figure 1 (b)
358 has been developed—moreover, the geometry has been meshed using 375907 elements. The
359 theoretically calculated primary resonance of the energy harvester was 29.687 Hz while the
360 experimentally obtained natural frequency was 28.27 Hz; furthermore, the theoretical
361 parametric resonance was calculated to be 59.374 Hz while the experimentally obtained
362 parametric was in the vicinity of 57.5 Hz—these results are within very good agreement of
363 each other. From theoretical simulations the maximum parametric motion amplitude occurred
364 at the centre of the beam as shown in Figure 10.



365 Figure 10: Theoretical mode shape of the fundamental and parametric resonance

366
367 Theoretical simulations for the frequency-response curves have also been done using
368 COMSOL Multiphysics to verify the experimentally obtained results at the fundamental
369 resonance as shown in Figure 11; results are within good agreement close to resonance

370 behaviour and post resonance, however, prior to $\Omega/\omega_1 \approx 0.98$ a discrepancy between the two
 371 results was obtained—this was due to the axial excitation resulting in a zero-response
 372 experimentally, however, results are within good agreement.



373 Figure 11: Comparison between theoretical and experimental results obtained at the fundamental resonance

374 5. Conclusions

375 An energy harvester has been designed, fabricated and tested, operating based on the
 376 nonlinear dynamical response of a parametrically excited clamped-clamped system using a
 377 beam with a point-mass (magnets) as the core element; as the core element resonates, the
 378 magnets pass through a coil to generate a backward electromotive force for energy
 379 harvesting. An electrodynamic shaker was used to excite the energy harvester and
 380 experiments have been conducted when the core element was excited (i) harmonically near
 381 the primary resonance; (ii) harmonically in the vicinity of the principal parametric resonance;
 382 (iii) in the vicinity of the principal parametric resonance with a non-smooth periodic

383 excitation. Experiments (i-iii) were used to evaluate the *increased operating bandwidth* of the
384 *nonlinear energy harvester*.

385 The magnets attached to the core element showed non-symmetric motion (hence energy
386 harvested) due to a small initial geometric imperfection; the parametric displacement was
387 larger in one direction about the initial equilibrium position. It was observed that when the
388 energy harvester was excited near the primary resonance, linear energy was harvested. When
389 the core element was excited in the vicinity of the principal parametric resonance, the
390 dynamics substantially changed; a strong softening-type nonlinearity was observed near
391 $\Omega/2\omega_1$ which was due to the effects of parametric excitations, nonlinearity and initial
392 geometric imperfection about the equilibrium position. In the vicinity of the principal
393 parametric resonance, the nonlinear energy harvested possesses two discontinuities (i.e.
394 saddle-node and period-doubling bifurcations); this nonlinear behaviour is advantageous in
395 broadening the frequency range at which the energy is harvested—the motion amplitude was
396 also larger than its linear counterpart at the primary resonance. With a non-smooth periodic
397 excitation in the vicinity of the principal parametric resonance, the system performed best,
398 displaying the largest motion amplitude and the energy harvested as well as *effective*
399 *operating bandwidth*; the energy harvester displayed a period-2 motion. For the theoretical
400 investigation, the calculated fundamental and parametric resonances are within very good
401 agreement of each other; moreover, the theoretical frequency-response curves are also within
402 good agreement of the experimental results.

403 It was observed that the system harvests energy at both the primary and principal
404 parametric resonances (displaying strong softening-type nonlinearity at the principal
405 parametric resonance); the *parametric* design has substantial *qualitative* and *quantitative*
406 effects on the *nonlinear dynamical response*, hence *increasing* the amount of *energy*
407 *harvested* and *effective operating bandwidth* of the device.

408 **References**

- 409 1. Saadon, S. and O. Sidek, *A review of vibration-based MEMS piezoelectric energy harvesters.*
 410 Energy Conversion and Management, 2011. **52**(1): p. 500-504.
- 411 2. Adhikari, S., M.I. Friswell, and D.J. Inman, *Piezoelectric energy harvesting from broadband*
 412 *random vibrations.* Smart Materials and Structures, 2009. **18**(11).
- 413 3. Renno, J.M., M.F. Daqaq, and D.J. Inman, *On the optimal energy harvesting from a vibration*
 414 *source.* Journal of Sound and Vibration, 2009. **320**(1–2): p. 386-405.
- 415 4. Fan, K.-Q., et al., *Design and experimental verification of a bi-directional nonlinear*
 416 *piezoelectric energy harvester.* Energy Conversion and Management, 2014. **86**: p. 561-567.
- 417 5. Fan, K., et al., *Design and development of a multipurpose piezoelectric energy harvester.*
 418 Energy Conversion and Management, 2015. **96**: p. 430-439.
- 419 6. Guan, M. and W.-H. Liao, *Design and analysis of a piezoelectric energy harvester for*
 420 *rotational motion system.* Energy Conversion and Management, 2016. **111**: p. 239-244.
- 421 7. Bu, L., et al., *Non-resonant electrostatic energy harvester for wideband applications.* IET
 422 Micro Nano Letters, 2013. **8**(3): p. 135-137.
- 423 8. Sardini, E. and M. Serpelloni, *An efficient electromagnetic power harvesting device for low-*
 424 *frequency applications.* Sensors and Actuators A: Physical, 2011. **172**(2): p. 475-482.
- 425 9. Marin, A., et al., *Broadband electromagnetic vibration energy harvesting system for*
 426 *powering wireless sensor nodes.* Smart Materials and Structures, 2013. **22**(7).
- 427 10. Ooi, B.L. and J.M. Gilbert, *Design of wideband vibration-based electromagnetic generator by*
 428 *means of dual-resonator.* Sensors and Actuators A: Physical, 2014. **213**: p. 9-18.
- 429 11. Siddique, A.R.M., S. Mahmud, and B.V. Heyst, *A comprehensive review on vibration based*
 430 *micro power generators using electromagnetic and piezoelectric transducer mechanisms.*
 431 Energy Conversion and Management, 2015. **106**: p. 728-747.
- 432 12. Roundy, S. and Y. Zhang. *Toward self-tuning adaptive vibration-based microgenerators.* in
 433 *Proc. SPIE.* 2005.
- 434 13. Williams, C.B. and R.B. Yates, *Analysis of a micro-electric generator for microsystems.*
 435 Sensors and Actuators A: Physical, 1996. **52**(1–3): p. 8-11.
- 436 14. Mitcheson, P.D., et al., *Architectures for vibration-driven micropower generators.* Journal of
 437 Microelectromechanical Systems, 2004. **13**(3): p. 429-440.
- 438 15. Stephen, N.G., *On energy harvesting from ambient vibration.* Journal of Sound and Vibration,
 439 2006. **293**(1–2): p. 409-425.
- 440 16. Shahruz, S.M., *Design of mechanical band-pass filters with large frequency bands for energy*
 441 *scavenging.* Mechatronics, 2006. **16**(9): p. 523-531.
- 442 17. Tang, X. and L. Zuo, *Enhanced vibration energy harvesting using dual-mass systems.* Journal
 443 of Sound and Vibration, 2011. **330**(21): p. 5199-5209.
- 444 18. Erturk, A. and D.J. Inman, *On mechanical modeling of cantilevered piezoelectric vibration*
 445 *energy harvesters.* Journal of Intelligent Material Systems and Structures, 2008. **19**(11): p.
 446 1311-1325.
- 447 19. Leland, E.S. and P.K. Wright, *Resonance tuning of piezoelectric vibration energy scavenging*
 448 *generators using compressive axial preload.* Smart Materials and Structures, 2006. **15**(5).
- 449 20. Eichhorn, C., F. Goldschmidtboeing, and P. Woias, *Bidirectional frequency tuning of a*
 450 *piezoelectric energy converter based on a cantilever beam.* Journal of Micromechanics and
 451 Microengineering, 2009. **19**(9).
- 452 21. Mann, B.P. and N.D. Sims, *Energy harvesting from the nonlinear oscillations of magnetic*
 453 *levitation.* Journal of Sound and Vibration, 2009. **319**(1–2): p. 515-530.
- 454 22. Maiorca, F., et al., *Diode-less mechanical H-bridge rectifier for “zero threshold” vibration*
 455 *energy harvesters.* Sensors and Actuators A: Physical, 2013. **201**: p. 246-253.

- 456 23. Liu, H., et al., *Investigation of a MEMS piezoelectric energy harvester system with a*
457 *frequency-widened-bandwidth mechanism introduced by mechanical stoppers*. Smart
458 Materials and Structures, 2012. **21**(3).
- 459 24. Sebald, G., et al., *Experimental Duffing oscillator for broadband piezoelectric energy*
460 *harvesting*. Smart Materials and Structures, 2011. **20**(10).
- 461 25. Masana, R. and M.F. Daqaq, *Response of duffing-type harvesters to band-limited noise*.
462 Journal of Sound and Vibration, 2013. **332**(25): p. 6755-6767.
- 463 26. Halvorsen, E., *Fundamental issues in nonlinear wideband-vibration energy harvesting*.
464 Physical Review E - Statistical, Nonlinear, and Soft Matter Physics, 2013. **87**(4).
- 465 27. Abdelkefi, A., A.H. Nayfeh, and M.R. Hajj, *Global nonlinear distributed-parameter model of*
466 *parametrically excited piezoelectric energy harvesters*. Nonlinear Dynamics, 2012. **67**(2): p.
467 1147-1160.
- 468 28. Daqaq, M.F., et al., *Investigation of power harvesting via parametric excitations*. Journal of
469 Intelligent Material Systems and Structures, 2009. **20**(5): p. 545-557.
- 470 29. Mann, B.P. and N.D. Sims, *On the performance and resonant frequency of electromagnetic*
471 *induction energy harvesters*. Journal of Sound and Vibration, 2010. **329**(9): p. 1348-1361.
- 472 30. Elvin, N.G. and A.A. Elvin, *An experimentally validated electromagnetic energy harvester*.
473 Journal of Sound and Vibration, 2011. **330**(10): p. 2314-2324.

474